STEPHEN J. POWERS

MRI PHYSICS

TECH TO TECH EXPLANATIONS

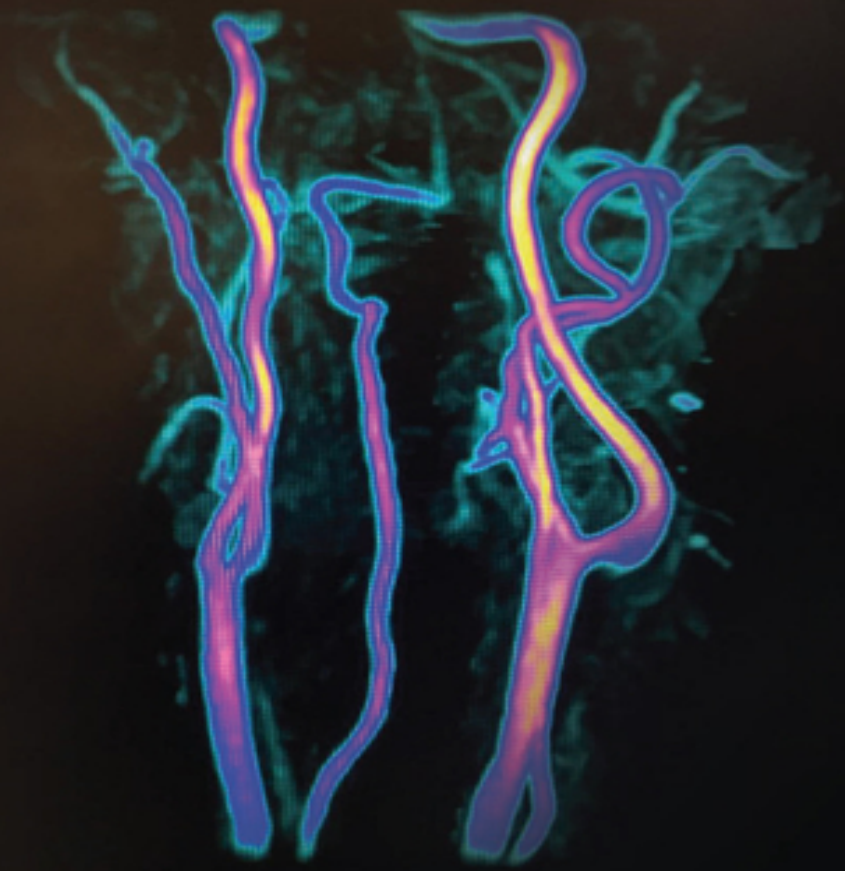

WILEY Blackwell

Table of Contents

- Cover
- Title Page
- Copyright Page
- Dedication Page
- About the Author
- Preface
  - Disclaimer
- Acknowledgements
- Introduction
  - Safety
  - Your Point of View While You Are Scanning
  - The MR Experiment in Images
- 1 Hardware: Magnet Types and Coils
  - Magnets
  - Coils
- 2 The Basics
  - Why the Hydrogen Molecule?
  - The Net Magnetization Vector
  - MRI is a Sequence of Events
  - Free Induction Decay (FID)
  - Relaxation
  - Proton Density
  - Image Contrast
  - The IQ Triangle: Contrast, SNR, Resolution
  - B_0 and B1

Free and Bound Protons
3 Image Weighting
Where Does Image Weighting Come From?
Time of Repetition (TR)
Time of Echo (TE)
TE and TR
Why Different TR Ranges for Different Field Strengths?
How Does TR Control T1?
What Does TR Affect?
Interpreting the T1 Relaxation Curve
Time of Repetition: Effects of the TR
TE: The T1 and T2 of it
Interpreting the T2 Relaxation Curve
Effects of TE on Image Contrast
What Do the Lines on the Curves Really Mean Anyway?
One Last Weighting Triangle
T1 and T2 Contrast Review
4 Introduction to the Basic Pulse Sequences
What is a Pulse Sequence?
Spin Echo (SE)
Gradient Echo/Gradient Recalled Echo (GRE)
Line Diagram Anatomy
The Ernst Angle
5 Multi Echo Spin Echo Sequence
Introduction to *k*-Space
k-Space: Phase Encoding
With FSE, Watch the Speed Limit!

k-Space, ETL, and Image Contrast
Filling *k*-Space
Pros and Cons of FSE
Another Way to View T2* and 180°s
Where Do Relaxation and Decay Curves Come From?
A T2* Curve Compared to the T2 Curve
Metal Artifact Reduction (MARS)
Driven Equilibrium: A “Forced T1”
3D FSE: CUBE/SPACE/VISTA
Single Shot FSE/HASTE
6 Tissue Suppression
Tissue Saturation versus Suppression
Inversion Recovery – Part One: STIR
Inversion Recovery: STIR with Vectors
Inversion Recovery Part Two: T2 FLAIR
IR Sequences: T1 and T2 FLAIR
IR Weightings: STIR, T1 and T2 FLAIR
Inversion Recovery – Part Two
The Rupture View
Tissue Saturation: Chemical Shift
Chemical Saturation at Low Fields
Tissue Saturation: SPAIR and SPIR
The Dixon Technique
Water Excitation
Saturation Pulses or Bands
Subtractions
Magnetization Transfer

IR Prepped Sequences
How is an RF Pulse Selective or Non-Selective?
Water Excitation Sequences
7 The Gradient Echo Sequence
GRE Sequence Structure
Phase Dispersion and Gradient Reversal
Analog to Digital Converter (ADC)
GRE Sequence Image Weighting
Two Different Kinds of T2 Relaxation
The GRE Weighting Triangle
GRE and SE Differences
Different Gradient Echo Types
In and Out of Phase TEs
In Phase/Out of Phase at 1.5 T
8 Gradient Echo Magnetic Resonance Angiography
Time of Flight MRA
TOF Angiography: Two Golden Rules
Types of MRA Sequences
TOF Concept in MRA versus MRV
2D versus 3D
2D TOF MRAs
3D TOF MRAs
In-Plane Saturation
In-Plane Saturation Avoidance
Magnetization Transfer (MT)
Options for Better MRAs
Phase Contrast MRA
9 *k*-Space

What Is Fourier Transform?
k-Space Filling
10 Echo Planar Sequences
Diffusion Weighted Imaging
Diffusion Tensor Imaging or White Matter Tractography
Susceptibility Weighted Imaging
Brain Perfusion
Arterial Spin Labeling
Spectroscopy
11 Geometric Parameters
Field of View (FOV) Is Your Film Size
Nex, ACQ, NSA, and SNR
Scan Matrix
Frequency Matrix
Echo Train Length
Echo Spacing
Echo Train Balancing
Slice Thickness and Slice Gap
Fractional Echo
Bandwidth
Rectangular (Rec.) FOV
No Phase Wrap/Phase Oversampling/Fold-Over Suppression
Concatenations or Acquisitions
Sequential Order Acquisition
12 Image Artifacts
Motion
Flow Artifact/Phase Mis-registration

RF Artifacts
Wrap/Aliasing/Fold-over Artifact
Gibbs Artifact (Ringing/Truncation)
Chemical Shift Artifact
Cross-talk
Cross-excitation
Gradient Warp or Distortion
Metal Artifacts
Corduroy Artifact
Annifact
Moiré Fringe Artifact or Zebra Artifact
Magnetic Susceptibility Artifact
Dielectric Effect or Standing Wave
Magic Angle Artifact
13 Gradients
Physical Gradients
Logical Gradients
14 MRI Math
The Larmor Equation: $W_0 = \gamma B_0$
Acquisitions or Nex or NSA
Scan Time Equations
Pixel Size and Voxel Volume
How to Convert Hz per Pixel to MHz
In and Out of Phase TEs
Dixon Method or Technique
SNR and the 3D Sequence
15 Parallel Imaging
Parallel Imaging: What Is It?

When and Where to Use the Speed
Parallel Imaging: How Does It Work?
Parallel Imaging: Pros and Cons
16 IV Gadolinium
Why We Use Gad
How Does Gad Shorten the T1 of Tissues?
The Blood–Brain Barrier
Post Contrast T2 FLAIR Imaging
Imaging Gadolinium
Eovist®
Glossary
Suggested Reading
Books
Videos
Index
End User License Agreement

List of Tables

Chapter 8
Table 8.1 What the different flow types look like.

List of Illustrations

Introduction
Figure I.1 Beware: Not all stretchers, IV poles, or O2 bottles are made of n...
Figure I.2 The 5 Gauss line. Diagram of a scan room.

Figure I.3 The 5 Gauss line. A scan room floor.

Figure I.4 Street sign warning of a steep gradient.

Figure I.5 The electromagnetic spectrum. Radiofrequencies used by MRI are ci...

Figure I.6 Artifact caused by LED light bulb.

Figure I.7 The patient is head first and supine. Note that the coil is aroun...

Figure I.8 The net magnetic vector (NMV) is in the longitudinal (0°/180°) pr...

Figure I.9 T1 axial pre. A possible cyst (circled) is doing the “fluid” thin...

Figure I.10 **STIR Coronal.** A possible cyst (oval) doing the “fluid” thing. It...

Figure I.11 Two similar contrasts: Notice that T2 FS and STIR have dark fat ...

Figure I.12 T1 fat-sat pre. Pre contrast done immediately before administrat...

Figure I.13 T1 fat-sat post gadolinium. The post contrast image shows slight...

Chapter 1

Figure 1.1 The four basic coil types. Typical body parts they are used on ar...

Figure 1.2 Shoulder coil or Helmholtz pair on the right. An x-ray of that sa...

Figure 1.3 Typical knee and head coils.

Figure 1.4 An inherent T/R body coil.

Chapter 2

Figure 2.1 The net magnetization vector (NMV).

Figure 2.2 You are looking from the side of the scanner. Many small vectors ...

Figure 2.3 The NMV aligned with the magnetic field (0/180) waiting to be exc...

Figure 2.4 The excitation pulse moves the NMV into the transverse or X/Y pla...

Figure 2.5 Top: The RF is “on”. All protons are in phase (all together) in t...

Figure 2.6 Top: The NMV while in the X/Y plane (here @90° to B0) rotate...

Figure 2.7 Top: Here the 180° RF has flipped the vectors to the other side a...

Figure 2.8 Protons diphase, then are flipped over as result of the 180°RF an...

Figure 2.9 The decaying of phase (T2* or FID) after the RF pulse is shut off...

Figure 2.10 After the FID, a 180° RF causes a **Spin Echo** to form. In answer t...

Figure 2.11 Top: The dotted T2* curve is a realistic curve having no 180°s c...

Figure 2.12 The IQ triangle.

Figure 2.13 The same slice in the same patient. Left: Nice T1 contrast: good...

Figure 2.14 Different image contrasts demonstrated. T1: High signal intensit...

Figure 2.15 Top (brain): Left: TR 217 ms, 10 ms TE. Low SNR, good T1 contras...

Figure 2.16 Signal and noise.

Figure 2.17 Both sine waves are superimposed to show the idea of how much si...

Figure 2.18 Left: High spatial resolution: pixel dimensions 320 × 320. Right...

Figure 2.19 PD coronal knee, T1 sagittal ankle, and PD fat saturated wrist. ...

Chapter 3

Figure 3.1 The “weighting triangle.” MRI can produce only three weightings: ...

Figure 3.2 A Pulse Sequence Design (PSD). The TR is the time interval (in ms...

Figure 3.3 A PSD showing the TE as the time from excitation to the center of...

Figure 3.4 T1 contrast curve diagram.

Figure 3.5 Image 1. There is low SNR due to saturation. The image has good T...

Figure 3.6 Larger images for better visualization, taken at five different T...

Figure 3.7 Typical T2 curves representing signal intensity difference. The d...

Figure 3.8 Image 1 – PD. CSF is not so bright. Some white matter (WM)/grey m...

Figure 3.9 Figures 3.5 and 3.7 side by side for comparison.

Figure 3.10 The short TR maximizes T1 so fat, gadolinium, and proteins will ...

Figure 3.11 White Matter (WM)/Grey Matter (GM) differentiation.

Chapter 4

Figure 4.1 A spin echo line diagram in its simplest form. The classic charac...

Figure 4.2 A basic PSD, as seen in Figure 4.1. TR is displayed as beginning ...

Figure 4.3 The same basic PSD as in Figures 4.1 and 4.2. Note the position o...

Figure 4.4 Susceptibility is demonstrated in the right frontal area (arrows)...

Figure 4.5 The CSE sequence. 1. A 90° **RF** pulse and a slice select gradient **(**...

Figure 4.6 A simplified example of a gradient echo PSD.

Figure 4.7 The GRE sequence. 1. The slice select gradient (SSG) and an RF pu...

Figure 4.8 A T1 curve of two different tissues. This diagram shows the signa...

Figure 4.9 The Ernst angle is easy to take advantage of. On **2D** Time of Fligh...

Chapter 5

Figure 5.1 A multi echo (FSE/TSE) sequence.

Figure 5.2 The center zone of *k*-space contributes close to 90% of an image’s...

Figure 5.3 The phase encoding gradient (PEG).

Figure 5.4 A weak amplitude PEG is applied to the first echo (ETE), putting ...

Figure 5.5 A low amplitude PEG is applied to the later echo (ETE) so it will...

Figure 5.6 *k*-Space is filled with ETE (10 ms) placed in the center by weak P...

Figure 5.7 *k*-Space is filled as shown in Figure 5.5. The ETE (30 ms) is plac...

Figure 5.8 If the ETE is 10 ms, then the other four TEs will outweigh the fi...

Figure 5.9 Taken at 3 T. Left. A 3 ETE of TE 10 ms. Decent T1 contrast, dark...

Figure 5.10 A very simplified depiction of a *k*-space. The scan matrix is 9 ×...

Figure 5.11 An FSE PSD with ETL of four. The 90° is followed by T2*, a 180° ...

Figure 5.12A A T2* decay curve.

Figure 5.12A, B A. A T2* decay curve. B. A T2 decay curve.

Figure 5.13 An FSE PSD with a driven equilibrium (DE) complex applied at the...

Figure 5.14 Top. **T2 axials** (split screen). Same patient, scan factors, and w...

Figure 5.15 Image obtained from 3D axial FSE, commonly known as “CUBE” or “S...

Figure 5.16 and 5.17 *k*-Space is symmetrical and is a mirror image of itself,...

Figure 5.18 Half-Fourier *k*-space filling. A little more than half of the lin...

Figure 5.19 The effect on resolution and SNR with increasing half or partial...

Figure 5.20 SSPSD. A single 90–180° RF pulse excites a slice. PEG is “blippe...

Figure 5.21 Trajectory *k*-space filling in SSFSE. Note lines of *k*-space filli...

Figure 5.22 Coronal T2 weighted SSFSE.

Chapter 6

Figure 6.1 A basic IR PSD. What is happening during the TI is T1 relaxation....

Figure 6.2 The NMVs shown are **pre** 180° inversion pulse. The dashed arrow rep...

Figure 6.3 NMVs **post** 180° RF. On the right, looking up the bore, NMV is poin...

Figure 6.4 During the TI, fat T1 relaxes to the null point with water pretty...

Figure 6.5 After the of the TI, a 90° is applied to the slice, driving fat (...

Figure 6.6 The 180° is the final RF pulse applied to the slice, driving fat ...

Figure 6.7 Remember, the 90°/270° position is the transverse plane, and the ...

Figure 6.8 Two STIR images. The one on the right was scanned at 1600 ms TR, ...

Figure 6.9 A pictogram of water and fat NMV positions from the RF pulses dur...

Figure 6.10 T2 FLAIR. CSF is dark and shows similar T2 contrast differences ...

Figure 6.11 STIR on the left, T2 axial on the right in the brain in the same...

Figure 6.12 Same slice, same patient. Left. The T1 FLAIR has dark CSF and go...

Figure 6.13 Left. Increased TI = darker, 220 ms. Right. Decreased TI = light...

Figure 6.14 Relaxation starts off at 180° and progresses towards the null po...

Figure 6.15 Two different implants. The one on the left is intact but with a...

Figure 6.16 Representations of the separation of the fat and water peaks (ch...

Figure 6.17 A series of same slice, same patient images at 1.5 T where all g...

Figure 6.18 The four different contrasts obtained with a Dixon sequence are:...

Figure 6.19 A spectrum with both peaks. The RF pulse that caused this spectr...

Figure 6.20 In water excitation, the RF has frequencies that only excite wat...

Figure 6.21 T2 fat-sat on the left and water excitation on the right. Both h...

Figure 6.22 An anteriorly placed saturation pulse (arrows). Here it is used ...

Figure 6.23 Example of a good subtraction with only very slight mis-registra...

Figure 6.24 Subtraction at mid to lower liver. The patient’s respiration was...

Figure 6.25 Three images of the same breast: Pre, post, and sub. **Note**: The r...

Figure 6.26 Sagittal abdominal MRA. Sub is on the right. Note loss of backgr...

Figure 6.27 Post liver on the left and its sub on the right. Note that paras...

Figure 6.28 Images of breast during biopsy. Note that the retro-areolar area...

Figure 6.29 I was gently shaking the handrail in a pool. The water acted to ...

Figure 6.30 Off center RF excites the slice; bound tissues transfer its magn...

Figure 6.31 A basic SE PSD with an MT pulse preceding the 90°.

Figure 6.32 A double IR sequence in the brain. Note that CSF is dark from th...

Figure 6.33 Three RF pulse playouts. See text for explanation.

Chapter 7

Figure 7.1 Road sign for a gradient.

Figure 7.2 Gradient A is opposed by an equal and opposite gradient, B. Any e...

Figure 7.3 Visual depiction of a loss of phase caused by a gradient, followe...

Figure 7.4 The RF and SSG are applied simultaneously with an opposite polari...

Figure 7.5 Analog wave form.

Figure 7.6 Split screen, same slice, same patient shows two different axials...

Figure 7.7 Using a higher F/A (50–90°), expect more T1 contrast; short TEs l...

Figure 7.8 A longer TE to more T2* contrast and a shallow/low F/A to decreas...

Figure 7.9 TR 567 ms, TE 10 ms, F/A 20°. This image has brighter fat, and be...

Figure 7.10 Same patient, same slices in GRE on the left and FSE on the righ...

Figure 7.11 On the left is an FSE with ETL of 23, and on the right is a GRE....

Figure 7.12 An SPGR PSD with the spoiler pulses circled.

Figure 7.13 A steady state GRE PSD with the re-winding a.k.a. re-phasing gra...

Figure 7.14 Note that the three Fs are bright: Fat, fluid, and flow. Having ...

Figure 7.15 A representation of two different pixels and the vectors present...

Figure 7.16 The progression in ms for IP/OOP TEs.

Figure 7.17 OOP and IP axials in the abdomen. Note the decrease in signal of...

Chapter 8

Figure 8.1 TOF MRAs tend to overestimate a stenosis (dashed lines).

Figure 8.2 SE images. On the left, blood is giving off a little signal as it...

Figure 8.3 Top, middle. The stationary tissue is darker than the flowing blo...

Figure 8.4 **Venous sat = MRA.** The figure shows venous blood (solid arrow) havi...

Figure 8.5 **Arterial sat = MRV.** This figure shows arterial blood (dashed arro...

Figure 8.6 A 3D GRE PSD. SSG is varied in amplitude, making the third dimens...

Figure 8.7 The image on the right shows the “stepping” artifact from the pat...

Figure 8.8 A single slab 3D with an inferior to superior ramp pulse (ramp pu...

Figure 8.9 The ideal angle (90° or perpendicular) of slice/slab position to ...

Figure 8.10 Note the carotid, middle right, has uniform signal through the e...

Figure 8.11 A ramped RF increases the F/A in the slab to counter blood satur...

Figure 8.12 Left. T1 axial imaging of the brain with and without MT. Right. ...

Figure 8.13 PSD of a PC sequence. Note that, in this example, the SSG is app...

Figure 8.14 A PC PSD. The NMVs for flow and stationary tissue are shown star...

Chapter 9

Figure 9.1 A *k*-space. The darker area is the "contrast" portion. Lines in th...

Figure 9.2 Linear filling (CSE or conventional GREs).

Figure 9.3 Re-ordered filling where, say, line #1 is filled first with the E...

Figure 9.4 Centric filling of *k*-space, in which the center lines are ideally...

Figure 9.5 A timing bolus run. Each slice is at a 2 s interval. This equates...

Figure 9.6 A coronal "Fluoro-Trigger" type image in the abdomen. Gadolinium ...

Figure 9.7 The "bolus track/care-bolus" method, where a "tracker" is placed ...

Figure 9.8 Elliptical centric *k*-space filling. Ideally, central lines are fi...

Figure 9.9 Elliptical centric *k*-space filling of the carotids. Inject in the...

Figure 9.10 The TRICKS/TWIST sequences are even more gradient intense than e...

Chapter 10

Figure 10.1 An EPI PSD with a string of gradient reversals and resulting ech...

Figure 10.2 A stripped-down PSD of a DWI sequence showing DW gradients, here...

Figure 10.3 Gradients for a low b-value on the left and high b-value on the ...

Figure 10.4 Acute CVA in the left parietal lobe; b-value 1000. Apparent diff...

Figure 10.5 A bladder diverticulum found during a prostate study. Note signa...

Figure 10.6 The image on the left is taken 1 min after the tea bags were pla...

Figure 10.7 Acute CVA on an ADC map, left, and the b-1000 DWI image right. S...

Figure 10.8 These images are same slice, same patient. There is a round lesi...

Figure 10.9 All four DWI images next to each other. Images are the same slic...

Figure 10.10 A. The many directions in a DTI sequence. Each “arm” in the orn...

Figure 10.11 You are looking for blood to cause a small local field inhomoge...

Figure 10.12 Multiple images of a sequence known as SWI, SWAN, and Venous BO...

Figure 10.13 A standard GRE next to a high resolution SWI.

Figure 10.14 Brain perfusion graphs (not for diagnostic purposes).

Figure 10.15 The graph shows the signal intensity of ROI #2 (right frontal) ...

Figure 10.16 Cerebral perfusion maps. Mean transit time (MTT) and time to pe...

Figure 10.17 The different phases or parts of an ASL sequence.

Figure 10.18 ASL image: Un-labeled on left, labeled in middle, and rCBV far ...

Figure 10.19 A fat-sat tuning spectrum on the left, and an actual spectrosco...

Figure 10.20 Spectroscopy showing peaks of the five most common metabolites....

Figure 10.21 Spectroscopy: Water contamination.

Figure 10.22 On the right is a good spectroscopy, on the left a poor spectro...

Figure 10.23 “Hunter’s angle” in brain spectroscopy.

Chapter 11

Figure 11.1 The image quality triangle, where contrast to noise (CNR) is the...

Figure 11.2 The FOV comes from the amplitude or “steepness” of the FEG. A st...

Figure 11.3 Noise (the dotted line) has a lower amplitude than the signal fo...

Figure 11.4 For the second nex, the amplitude of the noise is higher so SNR ...

Figure 11.5 An unbalanced echo train.

Figure 11.6 A balanced echo train. The ET has been adjusted to 20 so it now ...

Figure 11.7 A fractional or partial echo, where only about three quarters of...

Figure 11.8 In a narrow receiver B/W only the “sweet spot” (circled) of the ...

Figure 11.9 Three different transmitter B/Ws, all with the same center frequ...

Figure 11.10 A low and high amplitude SSG with the same B/W (63 ± 5) as in F...

Figure 11.11 Shows rectangular FOV applied in the phase direction (circled)....

Figure 11.12 This shows the area being “over-sampled” (circled), removing wr...

Figure 11.13 Slice wrap, seen on 3D sequences. The base of the skull anatomy...

Chapter 12

Figure 12.1 Note the time interval from phase encoding to the TE in SE. This...

Figure 12.2 Note the time interval from the Inversion Pulse to the TE in IR....

Figure 12.3 Motion artifact in phase direction on lumbar spine and sagittal ...

Figure 12.4 The motion suppression technique. Sections of *k*-space are sample...

Figure 12.5 The effects of gradient reversal on protons de-phased by the fir...

Figure 12.6 Two PSDs without and with flow comp. The TE lengthens due to the...

Figure 12.7 Two sagittal ankle STIR images, the right scanned without flow c...

Figure 12.8 RF artifact or zipper (dotted lines) from opening the scan room ...

Figure 12.9 Sine wave A is sampled according to the Nyquist theorem, which w...

Figure 12.10 The anterior aspect of the face is under sampled and displaced ...

Figure 12.11 Gibbs/Truncation artifact, cause 1: Anisotropic pixels on the l...

Figure 12.12 Gibbs/Truncation artifact, cause 2: Seen at high tissue contras...

Figure 12.13 Gibbs/Truncation artifact, cause 3: Asymmetric echo. Only part ...

Figure 12.14 Gibbs/Truncation artifact, cause 4: Varying SNR from line to li...

Figure 12.15 Gibbs/Truncation artifact, cause 4: Image windowed to demonstra...

Figure 12.16 Pixels are the dotted line. On the left, the pixel can hold all...

Figure 12.17 Both sets of images are windowed to demonstrate chem shift arti...

Figure 12.18 Two images of a fat-sat tuning spectrum. **Wide receiver B/W** on t...

Figure 12.19 IP (left) and OOP (right) echoes in the abdomen. The OOP on the...

Figure 12.20 Adjacent slices that have frequencies in common can interfere w...

Figure 12.21 The fix for “cross-talk” is to shift the slices away from each ...

Figure 12.22 An alternative fix for cross-talk is to interleave the slice ac...

Figure 12.23 Cross-excitation artifact: Dark bands on scouts in breast impla...

Figure 12.24 Cross-excitation: Overlapping of slices posterior to the spine....

Figure 12.25 Schematic showing the overlapping of slices causing the artifac...

Figure 12.26 Same slices and patient. Cross-excitation in T1s on the left, s...

Figure 12.27 Urinary bladder with cross-excitation.

Figure 12.28 The dashed line is the desired FOV. The solid line represents t...

Figure 12.29 Imaging past the linear portion of the gradient results in warp...

Figure 12.30 Another example of gradient warp (circled).

Figure 12.31 Metal artifact on scanning with three different sequences: SE, ...

Figure 12.32 Corduroy artifact. This comes from a data point or two which is...

Figure 12.33 Annifact.

Figure 12.34 Moiré fringe or zebra artifact.

Figure 12.35 Magnetic susceptibility from air in the paranasal sinuses. The ...

Figure 12.36 Right frontal hemorrhage on all weightings: A, GRE; B, T1 FSE; ...

Figure 12.37 Dielectric effect" (circled) in the same patient in two differe...

Figure 12.38 A simplified depiction of the dielectric effect. The large oval...

Figure 12.39 The patellar tendon at 55° to the main magnetic field (MMF) on ...

Figure 12.40 The dashed arrow points to the magic angle artifact (M.A.) in t...

Chapter 13

Figure 13.1 A photo of my **left** hand with the X, Y, and Z physical gradient d...

Figure 13.2 A magnet's strength comes from the amount of current flowing in ...

Figure 13.3 Z gradient, side view. The patient is silhouetted in the bore. T...

Figure 13.4 X gradient, side view. There are identical coils on opposite sid...

Figure 13.5 X gradient, sagittals. You are looking up the bore scanning sagi...

Figure 13.6 Y gradient, coronals. Coils at the top of the main magnetic fiel...

Figure 13.7 Y gradient seen from above. The patient is silhouetted supine in...

Figure 13.8 The gradient directions on this axial image of the brain were "s...

Figure 13.9 An FSE pulse sequence with an ET of 4. The Z gradient is slice s...

Figure 13.10 Same PSD as in Figure 13.9 with an ET of 4, but coronal slices....

Figure 13.11 SSG is applied, the top slice is excited with a 90° RF at 65 MH...

Figure 13.12 Five echoes, same frequency. Five different phases from five di...

Figure 13.13 The five PEGs vary in strength from high negative applications ...

Figure 13.14 A truncated PEG playout of steps: −127 to 0, and then out to ph...

Figure 13.15 A representation of the *k*-space for slice 5. In it we have a ph...

Chapter 14

Figure 14.1 Signal to noise changes with the square root of the number of ac...

Figure 14.2 The difference between isotropic and anisotropic voxels.

Figure 14.3 Think of a 3D slab as a big, thick slice. That slice is divided ...

Chapter 15

Figure 15.1 Left. Coil sensitivity maps. These provide information to undo t...

Figure 15.2 A *k*-space and how it is filled in the GRAPPA method. The center ...

Figure 15.3 Loss of overall SNR. Note graininess of the left image. The righ...

Figure 15.4 Same phantom, parameters, and slice. The right image has PI of 2...

Chapter 16

Figure 16.1 The “closeness” of the three curves tells us that all three tiss...

Figure 16.2 T1 curves post gad. Tumor (dashed line) shows distinct shortenin...

Figure 16.3 Left, pre gad. There is pathology in the left cerebellum (known ...

Figure 16.4 The first and second toes. Post gad image. The axial post gad im...

Figure 16.5 The first and second toes. Pre and post gad image. You know some...

Figure 16.6 Same slice, same patient. T2 fat-sat FLAIRs pre and post gad at ...

Figure 16.7 Same slice, same patient. At the level of the pineal gland, agai...

Figure 16.8 Top. Fat-sat T2 FLAIRs pre and post show gad enhancement inside ...

Figure 16.9 A phantom with three syringes containing different concentration...

Figure 16.10 A set of images from a shoulder arthrogram in which pure gad wa...

Figure 16.11 A shoulder radiograph/arthrogram using non-dilute gad. Gad is b...

Figure 16.12 Top. Arterial and venous liver with Eovist. Bottom. 15- and 20-...

Figure 16.13 MRCP images taken pre and post injection of Eovist. As previous...

MRI Physics

Tech to Tech Explanations

Stephen J. Powers, B.S.R.T. (R), (CT), (MR)
South Coast Hospital Group
Fall River, MA, USA

WILEY Blackwell

This edition first published 2021
© 2021 John Wiley & Sons Ltd

All rights reserved. No part of this publication may be reproduced, stored in a retrieval system, or transmitted, in any form or by any means, electronic, mechanical, photocopying, recording or otherwise, except as permitted by law. Advice on how to obtain permission to reuse material from this title is available at http://www.wiley.com/go/permissions.

The right of Stephen J. Powers to be identified as the author of this work has been asserted in accordance with law.

Registered Office(s)
John Wiley & Sons, Inc., 111 River Street, Hoboken, NJ 07030, USA
John Wiley & Sons Ltd, The Atrium, Southern Gate, Chichester, West Sussex, PO19 8SQ, UK

Editorial Office
9600 Garsington Road, Oxford, OX4 2DQ, UK

For details of our global editorial offices, customer services, and more information about Wiley products visit us at www.wiley.com.

Wiley also publishes its books in a variety of electronic formats and by print-on-demand. Some content that appears in standard print versions of this book may not be available in other formats.

Limit of Liability/Disclaimer of Warranty
The contents of this work are intended to further general scientific research, understanding, and discussion only and are not intended and should not be relied upon as recommending or promoting scientific method, diagnosis, or treatment by physicians for any particular patient. In view of ongoing research, equipment modifications, changes in governmental regulations, and the constant flow of information relating to the use of medicines, equipment, and devices, the reader is urged to review and evaluate the information provided in the package insert or instructions for each medicine, equipment, or device for, among other things, any changes in the instructions or indication of usage and for added warnings and precautions. While the publisher and authors have used their best efforts in preparing this work, they make no representations or warranties with respect to the accuracy or completeness of the contents of this work and specifically disclaim all warranties, including without limitation any implied warranties of merchantability or fitness for a particular purpose. No warranty may be created or extended by sales representatives, written sales materials or promotional statements for this work. The fact that an organization, website, or product is referred to in this work as a citation and/or potential source of further information does not mean that the publisher and authors endorse the information or services the organization, website, or product may provide or recommendations it may make. This work is sold with the understanding that the publisher is not engaged in rendering professional services. The advice and strategies contained herein may not be suitable for your situation. You should consult with a specialist where appropriate. Further,

readers should be aware that websites listed in this work may have changed or disappeared between when this work was written and when it is read. Neither the publisher nor authors shall be liable for any loss of profit or any other commercial damages, including but not limited to special, incidental, consequential, or other damages.

Library of Congress Cataloging-in-Publication Data

Names: Powers, Stephen J. (Senior MRI technologist), author.
Title: MRI physics : tech to tech explanations / Stephen J. Powers.
Description: Hoboken, NJ : Wiley-Blackwell, [2021] | Includes index.
Identifiers: LCCN 2020026624 (print) | LCCN 2020026625 (ebook) | ISBN 9781119615026 (paperback) | ISBN 9781119615057 (adobe pdf) | ISBN 9781119615040 (epub)
Subjects: MESH: Magnetic Resonance Imaging | Physics
Classification: LCC RC386.6.M34 (print) | LCC RC386.6.M34 (ebook) | NLM WN 185 | DDC 616.07/548–dc23
LC record available at https://lccn.loc.gov/2020026624
LC ebook record available at https://lccn.loc.gov/2020026625

Cover Design: Wiley
Cover Image: Courtesy of Stephen Powers

If you can’t explain it to a 6-year-old, you don’t understand it yourself.
Albert Einstein